A Multicenter Clinical Trial on the Diagnostic Value of Dual-Tracer PET/CT in Pulmonary Lesions Using 3′-Deoxy-3′-^{18}F-Fluorothymidine and ^{18}F-FDG

Jiahe Tian[1], Xiaofeng Yang[2], Lijuan Yu[3], Ping Chen[4], Jun Xin[5], Liming Ma[6], Huiru Feng[7], Yieyin Tan[1], Zhoushe Zhao[8], and Wenkai Wu[9]

[1]Department of Nuclear Medicine, The Chinese PLA General Hospital, Beijing, China; [2]Department of Nuclear Medicine, The People's Hospital of Xinjiang Uygur Autonomous Region, Urumuqi, China; [3]Department of Medical Imaging, The Tumor Hospital Affiliated to Harbin Medical University, Heilongjiang, China; [4]PET/CT Center, The 1st Affiliated Hospital of Guangzhou Medical University, Guanzhou, China; [5]Department of Radiology, The 2nd Affiliated Hospital of China Medical University, Shenyang, China; [6]Department of Nuclear Medicine, The Kunming General Hospital, Yunan, China; [7]Department of Nuclear Medicine, The General Hospital of Beijing Command, Beijing, China; [8]Health Care System, GE China, Beijing, China; and [9]Department of Nuclear Medicine, Cancer Hospital, Peking Union Medical College, Chinese Academy of Medical Sciences, Beijing, China

Some new radiotracers might add useful information and improve diagnostic confidence of ^{18}F-FDG imaging in tumors. A multicenter clinical trial was designed to investigate the diagnostic performance of dual-tracer (^{18}F-FDG and 3′-deoxy-3′-^{18}F-fluorothymidine [^{18}F-FLT]) PET/CT in pulmonary nodules. **Methods:** Fifty-five patients underwent dual-tracer imaging in 6 imaging centers using the same models of equipment and standardized protocols. The images were interpreted by a collective group of readers who were unaware of the clinical data. The diagnostic performance using either tracer alone or dual-tracers together, with or without CT, was compared. The histological diagnosis or clinical findings in a 12-mo follow-up period served as the standard of truth. **Results:** In 16 patients with malignant tumor, 16 with tuberculosis, and 23 with other benign lesions, the sensitivity and specificity of ^{18}F-FDG and ^{18}F-FLT were 87.5% and 58.97% and 68.75% and 76.92%, respectively. The combination of dual-tracer PET/CT improved the sensitivity and specificity up to 100% and 89.74%. The 3 subgroups of patients could be best separated when the ^{18}F-FLT/^{18}F-FDG standardized uptake value ratio of 0.4–0.90 was used as the threshold. **Conclusion:** By reflecting different biologic features, the dual-tracer PET/CT using ^{18}F-FDG and ^{18}F-FLT favorably affected the diagnosis of lung nodules.

Key Words: pulmonary nodules; ^{18}F-FDG; 3′-deoxy-3′-^{18}F-fluorothymidine; dual-tracer PET/CT; multicenter clinical trial

It has been known for years that ^{18}F-FDG PET is of little value in certain types of tumors in spite of its wide acceptance in clinical oncology. One of the major shortcomings of ^{18}F-FDG was its nonspecific uptake by some benign lesions (*1*). Therefore, several alternative PET tracers were developed and tried to complement ^{18}F-FDG. Among them 3′-deoxy-3′-^{18}F-fluorothymidine (^{18}F-FLT) is receiving greater interest because it is an analog of thymidine and its uptake reflects cellular proliferation. In vitro and in vivo studies had shown a higher uptake of ^{18}F-FLT by the proliferating tumors (*2,3*). In a study on non–small cell lung cancer, a correlation was found between ^{18}F-FLT uptake and MIB-1 monoclonal antibody cytochemical staining of nuclei (*4*). In another study, Buck et al related the increased ^{18}F-FLT uptake exclusively to malignant tumors (*5*). However, to the best of our knowledge, ^{18}F-FLT has not been investigated comprehensively in clinical settings. We recently conducted a randomized, blinded, prospective multicenter clinical trial (MCCT) on PET/CT of pulmonary nodules using both ^{18}F-FDG and ^{18}F-FLT. The aims of this trial were (a) to verify the diagnostic performance of ^{18}F-FDG, ^{18}F-FLT, and dual-tracer imaging, (b) to determine the possible clinical advantage of dual-tracer PET/CT, and (c) to test the reliability and objectivity of the diagnostic criteria established in the trial.

MATERIALS AND METHODS

General Description of Study

This 2-y multicenter clinical trial was designed by a special task group consisting of nuclear medicine physicians, statisticians, Good Clinical Practice (GCP) staff, and law workers. The first half-year was dedicated to the staff training, preparation and printing of data sheets, case reporting forms, standard of operational

protocol (SOP), and other documents. The clinical imaging and data analysis took place in the next 1.5 y. Seven medical centers participated in the trial. One center acted as the organizer, taking the responsibility for collecting, verifying, and centrally processing data. The other 6 centers imaged the patients. To ensure the integrity of the data and the objectivity of the evaluation, the images acquired and processed using the standardized protocols and quality control—as well as the data recorded in the normalized forms—were collected by the organizing center, where a workstation had been installed for centralized processing. The images were interpreted in a randomized, blinded, collective reading, and the consensus diagnosis was compared with the standard of truth. The study protocol had been approved by the regional or hospital medical ethic committees.

Patient Enrollment

Patients entered the study in a sequential order. The inclusion criteria included (a) radiologic evidence of a pulmonary nodule or nodules($\leq$3), (b) no definite diagnosis, (c) no specific treatment before the study, (d) no significant dysfunction or disorder of major organs as suggested by laboratory or clinical signs (e.g., blood glucose $<$ 6.16 mmol/L, alanine aminotransferase $<$ 40 U/L, and urea $<$ 7.50 mmol/L), (e) willingness to follow the study protocols and to give written consent for participation in the trial, and (f) possible clinical outcome expected within the foreseeable duration of follow-up. The age and sex of the patients were of no concern in this trial.

The exclusion criteria included (a) diagnosis already defined, (b) severely ill or with metabolic abnormalities such as hyperglycemia, (c) unlikely to comply with the study protocols, and (d) unable to provide necessary clinical data. A patient's data would be excluded from the final analysis if a question existed on the quality of either radiotracer or PET/CT scan or the diagnosis was still in doubt at the time of final collective image reading.

Equipments and Acquisition Parameters

A similar model of PET/CT scanner (Discovery ST; GE Healthcare) and the same kinds of cyclotron (MiniTrace; GE Healthcare) and synthesizer (TracerLab Fx$_{FN}$; GE Healthcare) were used for PET/CT and radiotracer production in this trial. An obligatory standardized quality-control program was followed by all imaging centers and was subject to the organizer's inspections. To protect the patients from undue radiation dosage, a low-dose CT scan was acquired with the following settings: 120 kV, 100~250 mAs with automatic adjustment, 0.8-s rotation, 1.25-mm collimation, and a pitch varied according to the geometry of the CT detector (4, 8, or 16 slices). The PET scanner has a 15.7-cm axial field width and a spatial resolution of 4-mm full width at half maximum at 1 cm from the center. PET images were acquired in 3-dimensional mode, with 2.5 min per bed and 3 or 4 bed positions covering the entire chest. In some cases, whole-body ^{18}F-FDG imaging was performed from the bottom of the pelvis to the chin. The images were reconstructed in a Fourier rebinning iterative algorithm. Delayed imaging with similar acquisition parameters was recommended whenever possible.

Radiopharmaceuticals

Both ^{18}F-FDG and ^{18}F-FLT were automatically synthesized in each imaging center. The raw materials and agents for the synthesis were purchased by the organizer from the same supplier and delivered to each center. Both syntheses and quality control for every preparation of the pharmaceuticals strictly followed the

SOPs and were subject to inspection. The labeling yield, radiochemical purity, and specific radioactivity of the product were checked and recorded after each production. The products had to meet certain criteria—for example, the radiochemical yield must be $>$10% and the radiochemical purity must be $>$95%, to be used for imaging.

Imaging Protocols

Each patient was imaged twice using ^{18}F-FDG and ^{18}F-FLT within 7 d. The order of ^{18}F-FDG or ^{18}F-FLT scanning of each patient was determined randomly by a binary code produced by a computer. The patient was asked to fast over 4 h and to rest for 15 min before administration of 300~400 MBq radioactive tracers. The images were acquired at 60min after injection. On the basis of the clinical situation and the patient's agreement, some patients had a delayed scan at 120 min after injection. Within 7 d, the whole procedure was repeated using the alternative radiopharmaceutical.

Image Interpretation

The CT images were displayed as 5-mm cross-axial slices. The morphologic features of the nodule(s) were checked—such as the size, density, cavity, calcification, notch on margin, spiculated margin or plural contraction, and so forth—and the CT value was assessed. The PET images were visually inspected with the maximum standardized uptake value (SUV$_{MAX}$) determined from a circular region of interest (ROI) over the entire lesion. The uptake of a lesion was also scored in the following manner. In the case of ^{18}F-FDG, 0 = no uptake; 1 = uptake lower than that of the mediastinum; 2 = uptake equal to or greater than that of the mediastinum but lower than that of the liver; 3 = obvious uptake higher than that of the liver; and 4 = very strong uptake. For ^{18}F-FLT, 0 = no uptake, 1 = barely visible uptake, 2 = uptake lower than half the value of the thoracic vertebrae, 3 = obvious uptake similar to that of the vertebrae, and 4 = very high uptake.

The differential threshold for malignancy was set as SUV$_{FDG}$ $\geq$ 2.5, score$_{FDG}$ $\geq$ 2 and SUV$_{FLT}$ $\geq$ 1.4, score$_{FLT}$ $\geq$ 1. A lesion would be classified as malignant if uptake of both ^{18}F-FDG and ^{18}F-FLT or SUV and score were above the threshold, and the uptake of ^{18}F-FLT was lower than that of ^{18}F-FDG.

In cases of $>$1 lesion, the maximum scores and SUVs assessed among all lesions were chosen as the representative ones. The results in this trial were presented thereafter on a patient basis rather than on a lesion basis.

Data Collection and Verification

The original copies of working sheet and data record for each patient were sealed individually and, along with each patient's image data, sent to the organizing center over the Internet or by means of a CD-ROM. All sets of the serially numbered forms were required to be sent back to the organizing center whether they were or were not used. No correction or modification was allowed on the original records. After completion of the trial, the following datasets were collected from every center:

- Two original copies of PET/CT working sheet, one for each imaging-session.
- Two packages of raw image data from the dual-tracer PET/CT imaging.
- The original follow-up records, with the date and type of surgical procedure and the pathologic diagnosis or the date and findings on follow-up.

- The original copies of radiopharmaceutical production sheet, with the information on the production, quality control, and the raw material and agents used for each synthesis.
- The signed consent form from every subject.
- A summary of all cases, successful or failed, with the relevant information and explanations.
- A summary of the execution of the MCCT by each imaging center.

A group of physicians, physicists, radiochemists, administrators, and inspectors in the organizing center verified all data before further processing. Any noncompliance with the MCCT protocols resulted in exclusion of the patient's data. Forty patients were eventually excluded from the final analysis because of unsatisfactory image quality (n = 5), failure in ^{18}F-FLT synthesis (n = 29), or incomplete follow-up data (n = 6). Only 55 patients passed the data verification in the final analysis.

Collective Image Reading

Two sessions of blinded, collective image reading were carried out in this trial. The first session was organized in the sixth month after the initiation of the trial with 3 independent readers who had a CT or PET professional background. The purpose of the first reading was to verify the interpretation criteria. The final reading session took place on completion of the trial with an expanded team of readers. Only the results of the final reading session were analyzed and reported in this article.

Nine readers took part in the final collective reading. Four had professional CT backgrounds and the other 5 had professional nuclear medicine backgrounds. All readers were responsible for the primary PET/CT image interpretation in their own imaging centers. They had 1~4 y working experience with PET/CT when the trial began.

In the collective reading, the images were reconstructed and assessed using the central workstation. Every patient's images were read 7 times using different strategies—^{18}F-FDG, ^{18}F-FLT, CT alone, ^{18}F-FDG + ^{18}F-FLT, ^{18}F-FDG + CT, ^{18}F-FLT + CT in pairs, and, finally, the combination of ^{18}F-FDG + ^{18}F-FLT + CT. In each round of reading, the present order of the patients' images was randomized and the heading of images was masked before viewing. The readers read all images unaware of any patient's information. The images were projected onto a screen. The display window and angles were adjusted as reader(s) requested assistance from an independent operator. No discussion was allowed among readers; each reader had to make his or her own judgment on each subject and score the images. The recording sheet of every reader was collected before the next round of reading. The imaging diagnosis was determined by a consensus reached by at least 5 of 9 readers, and the corresponding score was determined by averaging. A ratio of SUV_{FLT}/SUV_{FDG} was also calculated in the collective reading. On completion of the final collective reading, the data were available to the readers, and the results were statistically analyzed in light of the standard of truth.

Endpoint and Standard of Truth

The endpoint of this trial was determined as either the pathologic evidence obtained from surgical processes or the clinical conclusion derived from the therapeutic response or from imaging or laboratory findings in follow-up over 1 y after imaging. Therefore, the standard of truth was the histologic diagnosis or the validated clinical evidence derived at the end of 12-mo follow-up period.

Statistical Analysis

Commercial (SPSS11.0) and dedicated (MINITABLE for 6 Sigma; GE Healthcare) software packages were used for the statistical analysis. The comparison on the diagnostic performances of image interpretation strategies and the correlation between SUVs and scores were analyzed. A statistician took an active part in the design, data check, and final analysis in this trial.

RESULTS

Clinical Trial

The first patient in this MCCT was imaged in January 2006, and the follow-up of the last patient was completed by June 2007. Among 55 patients entering the final analysis (Table 1), 33 were males and 22 were females (age range, 17- to 82-y-old). There were 28 patients with a solitary pulmonary nodule and 27 with 2 or 3 nodules. The size of the nodules ranged from 6 to ~110 mm, with the majority of lesions < 30 mm (n = 35). Because the 6 imaging centers covered wide geographic areas in China, with populations of different living habits and environment, the underlining diseases of our subjects were quite heterogeneous. The final diagnosis included 16 lung cancers, 16 tuberculoses, and 23 other benign lesions (inflammation, pseudotumor, granuloma, and other benign conditions). The diagnosis was confirmed via surgical processes (operation or biopsy) in 27 patients or via other clinical processes in 28 patients. No side effects were reported with either radiopharmaceutical or in PET/CT scanning.

^{18}F-FDG Images

A positive uptake of ^{18}F-FDG was noted in nearly all lesions (Fig 1A). The uptake varied in intensity, with a SUV_{MAX} of 0.75~16.0 and corresponding scores of 0~4. The mean SUV ± SD in patients with a malignancy (n = 16) was 8.13 ± 3.69 (range, 2.0~16.0), and the score was 3.12 ± 0.86 (range, 1.22~4.0), higher than that of tuberculoses (TB) (n = 16) and other benign diseases (n = 23). The corresponding values in the latter 2 groups were 5.71 ± 2.90 (range, 1.24~12.79), 2.73 ± 0.70 (range, 0.89~3.89), and 4.71 ± 0.74 (range, 0.75~16.0), 1.96 ± 1.33 (range, 0.61~4.0), respectively. ANOVA revealed a significant difference between groups in both SUV ($F_{2,52}$ = 4.583, P = 0.015) and score ($F_{2,52}$ = 6.338, P = 0.006). The Games–Howell test suggested that significant difference existed only between tumor and other benign lesions in both SUV (P = 0.021) and score (P = 0.005). There was a nonlinear correlation between the ^{18}F-FDG SUV_{MAX} and the ^{18}F-FDG scores (r^2 = 0.51, P = 0.000; Fig. 2).

^{18}F-FLT Images

In general, the uptake of ^{18}F-FLT by a pulmonary lesion was lower than that of ^{18}F-FDG (Fig. 1B). The higher uptake by liver and bone marrow of vertebrae and ribs made the detection of small lesion(s) by ^{18}F-FLT more difficult. The SUV_{MAX} and scores in malignancies were 3.54 ± 1.98 (range, 0.9~9.40) and 1.64 ± 1.14 (range, 0~3.81). The values in TB were 1.65 ± 0.99 (range, 0~3.3)

TABLE 1
Summary of Subjects

Patient	Sex	Age (y)	No. of nodules	Size (mm)	Diagnosis	SUV$_{FDG}$	SUV$_{FLT}$	FLT/FDG
1	F	42	1	20 × 21	Ad	9.7	4.13	0.43
2	F	53	2	20 × 20	TB	4.45	2.23	0.50
3	M	29	3	22 × 23	TB	5.8	2.3	0.40
4	F	17	3	37 × 49	TB	7	2.68	0.38
5	F	44	2	10 × 10	SN	3	4.2	1.40
6	M	38	3	30 × 50	TB	4.8	1.6	0.33
7	M	81	2	15 × 32	Ad	10.9	9.4	0.86
8	M	45	1	15 × 10	SN	6.56	2.04	0.31
9	M	76	1	25 × 15	Sq	8	3.8	0.48
10	F	48	2	29 × 41	IN	2.2	0.8	0.36
11	F	46	3	19 × 33	GN	3.6	1.32	0.37
12	F	65	1	15 × 14	TB	5	1.3	0.26
13	M	32	2	NA	TB	4	1.4	0.35
14	M	58	2	8 × 10	Ad	2	0.9	0.45
15	M	69	3	28 × 26	Ad	10.8	4.6	0.43
16	F	73	1	17 × 12	SN	2.2	2.2	1.00
17	M	35	3	26 × 23	TB	7.1	1.33	0.19
18	M	40	3	35 × 33	WG	16	4.73	0.30
19	M	46	1	15 × 26	TB	1.24	0	0
20	M	58	1	19 × 18	Ad	5	2.5	0.50
21	M	68	1	15 × 20	SN	1.9	0.5	0.26
22	M	43	3	25 × 31	TB	12.79	3.3	0.26
23	M	68	1	20 × 30	SN	11.06	5.1	0.46
24	M	63	2	70 × 40	IN	3.9	4.4	1.13
25	F	60	1	55 × 40	TB	3.02	1.11	0.37
26	F	37	2	25 × 30	MT	6	2.7	0.45
27	M	31	1	15 × 20	SN	3.92	1.42	0.36
28	F	35	1	NA	TB	3.8	1.47	0.39
29	F	43	1	10 × 10	SN	0.75	0.87	1.10
30	F	71	3	35 × 40	IN	8	3.1	0.39
31	M	50	1	75 × 110	Ad	16	4.73	0.30
32	M	64	1	12 × 13	Ad	3.7	1.7	0.46
33	M	46	3	55 × 40	BA	10	3.1	0.31
34	F	59	1	15 × 20	SN	7	0	0
35	F	67	1	15 × 10	TB	3.9	0	0
36	F	53	2	22 × 30	BA	7.3	2.9	0.40
37	M	66	2	11 × 13	IN	1.6	2.1	1.31
38	M	70	2	25 × 30	Ad	6	3.2	0.53
39	M	62	1	15 × 10	TB	4.1	1.4	0.34
40	M	71	2	45 × 38	Ad	10.5	4.3	0.41
41	M	82	1	NA	TB	10.2	3.2	0.31
42	F	58	1	23 × 23	SN	1.83	2.1	1.15
43	F	53	3	21 × 19	SN	1.9	1.8	0.95
44	M	36	2	15 × 20	IN	2	2.1	1.05
45	F	54	1	10 × 13	TB	8.78	2.4	0.27
46	F	49	1	20 × 10	GN	3.25	1	0.31
47	M	53	1	6 × 5	Ad	3	1.7	0.57
48	M	80	2	23 × 30	Sq	10	5	0.50
49	M	56	1	17 × 12	IN	7.7	0.32	0.04
50	M	76	2	28 × 20	SN	9.08	0.76	0.08
51	M	70	1	29 × 33	BA	11.24	2	0.18
52	M	77	1	61 × 28	TB	5.36	0.68	0.13
53	M	64	1	31 × 26	IN	5.78	3.4	0.59
54	F	35	3	18 × 13	SN	0.75	0.8	1.07
55	F	55	1	25 × 26	PT	4.2	0.42	0.10

Ad = adenocarcinoma; TB = tuberculosis; SN = stable nodule (no change after 1 y); Sq = squamous cancer; IN = inflammatory nodule (response to antibiotics); GN = granulomatous nodule; NA = not assessable; WG = Wegener's granuloma; MT = metastatic tumor; BA = bronchioalveolar carcinoma; PT = pseudotumor.
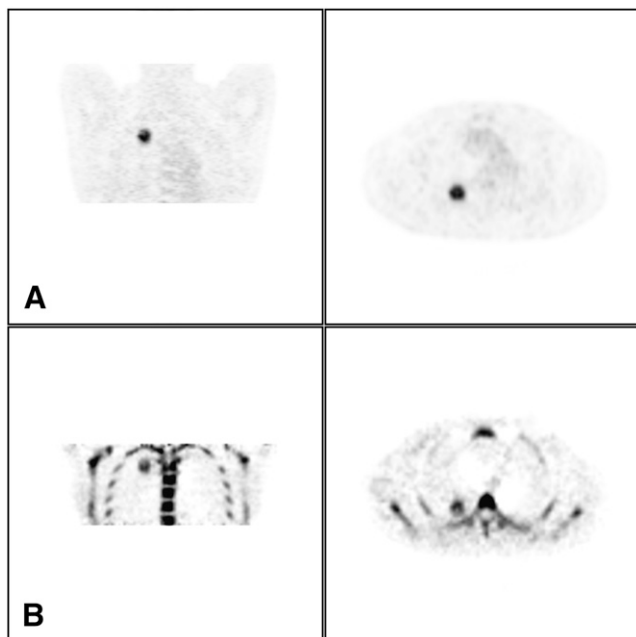
FIGURE 1. Patient 15 (male, 69-y-old) with adenocarcinoma of right lung (^{18}F-FDG/^{18}F-FLT = 0.43). (A) ^{18}F-FDG PET images are displayed in coronal and transaxial slices (SUV$_{MAX}$ = 10.8). (B) ^{18}F-FLT PET in the same patient (SUV$_{MAX}$ = 4.6). Difference on image quality was noticeable.

^{18}F-FLT and ^{18}F-FDG Ratios

Interestingly, the ratio between ^{18}F-FLT SUV$_{MAX}$ and ^{18}F-FDG SUV$_{MAX}$ (^{18}F-FLT/^{18}F-FDG) was found to be more accurate than any other criteria in the separation of different subgroups of patients (Fig. 4). Among 29 lesions with an ^{18}F-FLT/^{18}F-FDG ratio < 0.40, 14 were TB (Fig. 5), 12 were inflammation, and only 3 were malignant. All lesions with an ^{18}F-FLT/^{18}F-FDG ratio > 0.90 were inflammation (Fig. 6), whereas in 17 lesions with an ^{18}F-FLT/^{18}F-FDG ratio between 0.40 and 0.90, 13 were malignant. The difference in the ^{18}F-FLT/^{18}F-FDG ratio between the 3 subgroups was statistically significant (F$_{2,49}$ = 5.361, P = 0.008). The Games–Howell test indicated a significant difference between tumor and TB (0.45 ± 0.146 vs. 0.27 ± 0.140, P = 0.005) and between TB and other benign disease (0.61 ± 0.450, P = 0.007) but not between tumors and inflammation (P = 0.269), probably due to a rather large SD in the latter subgroup of patients.

Dual-Phase ^{18}F-FDG and ^{18}F-FLT Scans

Only 34 patients had delayed ^{18}F-FDG and 25 patients had delayed ^{18}F-FLT (n = 25) imaging. The change in the radiotracer uptake between early and delayed imaging varied unpredictably. In delayed ^{18}F-FDG imaging, 5 of 6 tumors, 9 of 12 TB, and 9 of 16 inflammations had their SUVs increased in delayed imaging, whereas decreased SUVs were noted in 1 of 6 tumors, 3 of 12 TB, and 4 of 16 inflammations. The mean ± SD of delayed SUV$_{FDG}$ was 8.97 ± 4.26 in tumor, 6.69 ± 3.04 in TB, and 4.76 ± 3.41 in inflammation. The ΔSUV was 24% ± 31%, 20.9% ± 35.3%, and 4.52% ± 26.95%, respectively. Increased ^{18}F-FLT$_{SUV}$ was noted in 3 of 7 tumors, 3 of 8 TB, and 2 of 10 inflammations. Four tumors, 5 TB, and 6 inflammations had decreased SUV$_{FLT}$ in delayed scanning. The delayed ^{18}F-FLT$_{SUV}$ was 4.18 ± 2.71, 1.59 ± 1.10, and 1.34 ± 0.91, and the ΔSUV was –0.09% ± 13.31%, –12.3% ± 20.48%, and 10.6% ± 41.35% in the 3 subgroups of patients, respectively. Statistically, no difference

and 1.21 ± 0.66 (range, 0~1.61), and in other benign lesions, the values were 1.56 ± 1.60 (range, 0–5.10) and 0.80 ± 0.81 (range, 0.44~2.17), respectively. ANOVA also indicated a significant difference among groups in SUV (F$_{2,52}$ = 7.119, P = 0.002) and score (F$_{2,52}$ = 6.786, P = 0.005). The Games–Howell test confirmed the significance of SUV difference between tumor, TB (P = 0.007), and other benign lesions (P = 0.033) but not between the 2 benign groups, whereas the score differed only between tumor and other benign diseases (P = 0.041). A linear correlation was noted between the ^{18}F-FLT SUV$_{MAX}$ and ^{18}F-FLT scores (r^2 = 0.59, P = 0.000; Fig. 3).
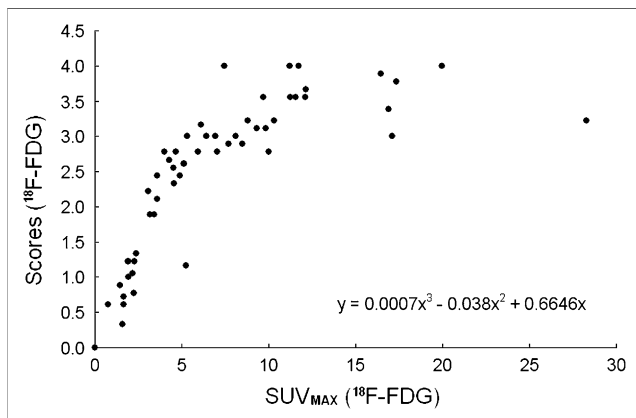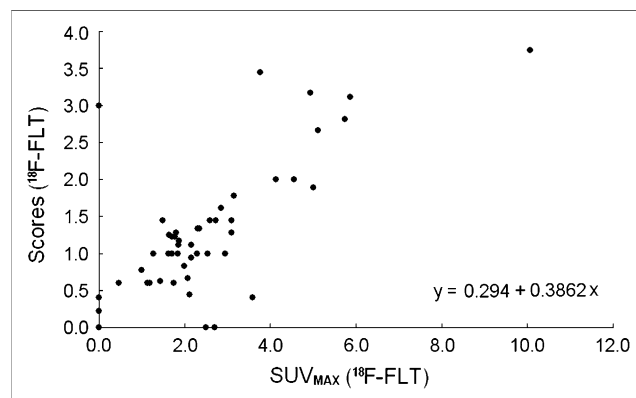

FIGURE 2. Nonlinear correlation existed between SUV$_{MAX}$ and scores of ^{18}F-FDG.

$$y = 0.0007x^3 - 0.038x^2 + 0.6646x$$

FIGURE 3. Linear correlation existed between SUV$_{MAX}$ and scores of ^{18}F-FLT.
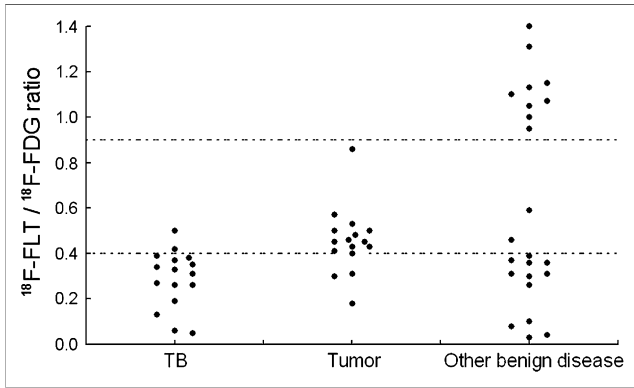
$$y = 0.294 + 0.3862x$$

FIGURE 4. Subgroups of patients with TB, tumor, and other benign diseases could be separated using an ^{18}F-FLT/^{18}F-FDG SUV ratio of 0.40~0.90. Thirteen of 16 tumors were in this range; only 2 TB and 2 inflammations were false-positive. Fourteen TB and 12 inflammations had ^{18}F-FLT/^{18}F-FDG ratios lower than 0.39. Nine patients had inflammatory lesions with ^{18}F-FLT/^{18}F-FDG ratios higher than 0.95.

in ΔSUV could be demonstrated between groups using either radiotracer.

Diagnostic Performance of Different Imaging Strategies

In the final collective image reading, ^{18}F-FDG PET correctly detected 14 of 16 malignant lesions. However, false-positive scans were noted in 16 of 39 benign cases. The sensitivity of ^{18}F-FLT PET was lower (11/16) and so was its false-positive rate (9/39). The low-dose CT alone had a diagnostic efficiency similar to that of ^{18}F-FLT (sensitivity, 11/16; specificity, 29/39). When the images were read in
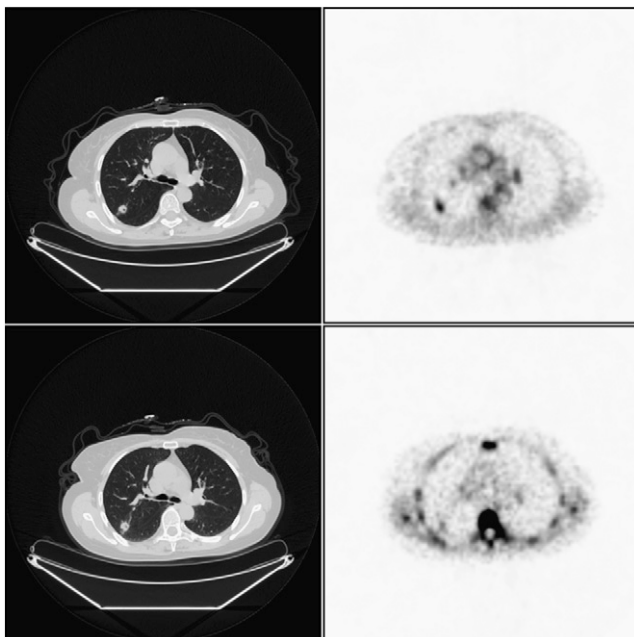

FIGURE 5. Patient 12 (female, 65-y-old) with 1.5 × 1.4 cm lesion at right upper lobe. Confirmed diagnosis was tuberculoses. SUV$_{FDG}$ = 5.0, SUV$_{FLT}$ = 1.3, and ^{18}F-FLT/^{18}F-FDG = 26%.

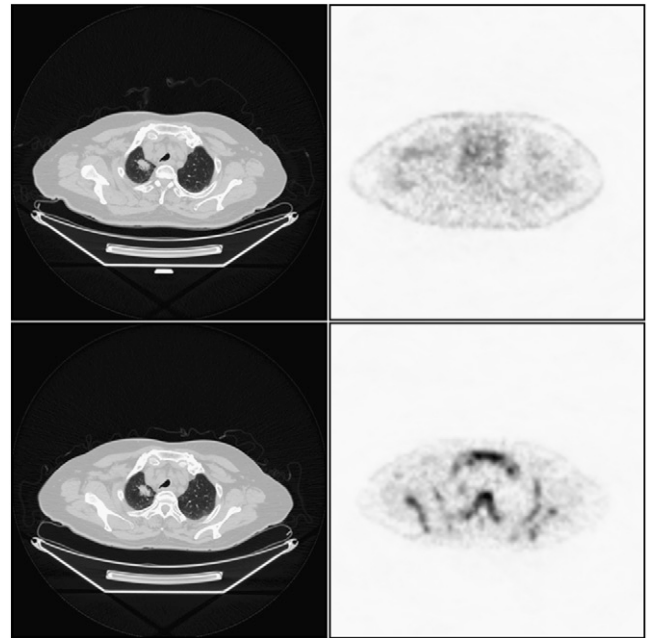**FIGURE 6.** Patient 16 (female, 73-y-old) with 1.7 × 1.2 cm confirmed inflammatory nodule in right upper lung. SUV$_{FDG}$ = 2.2, SUV$_{FLT}$ = 2.2, and ^{18}F-FLT/^{18}F-FDG = 100%.

pairs—such as ^{18}F-FDG + CT, ^{18}F-FLT + CT, or ^{18}F-FDG + ^{18}F-FLT—the specificity improved, especially when ^{18}F-FLT was read with ^{18}F-FDG. CT showed its value in cases of solitary pulmonary nodule (SPN) < 10 mm or with very low uptake when reading became more difficult. The diagnostic performance was obviously improved when the 3 sets of images were read together, resulting in the highest sensitivity, specificity, and accuracy (Table 2). The χ^2 test based on expected correct–wrong reading suggested that at least 1 strategy had an important influence on the overall diagnostic performance ($\chi^2 = 18.225$, $P = 0.006$) and that the paired ^{18}F-FDG + ^{18}F-FLT had the highest correct reading over other strategies; therefore, this strategy probably had the highest contribution to the interpretation accuracy (Table 3).

Cases with False Result

The data of 3 patients with lung malignancy were misinterpreted as benign in the collective reading. All were males (age range, 46- to 70-y-old). Bronchioalveolar cell carcinoma was pathologically proven in 2 patients. Careful reevaluation of the other case found an out-of-record "anti-tumor" therapy of unknown nature before the patient entered the study; therefore, the therapeutic effect on his lesions at the time of imaging could not be excluded.

False-positive results were encountered in 2 inflammatory nodules and 2 tuberculoses. One patient underwent surgery on the basis of the ^{18}F-FLT/^{18}F-FDG PET result, to confirm a lesion of TB. The other patient with TB responded to anti-TB treatment. The lesions of other 2 patients revealed no change in follow-up without antitumor treatment.

TABLE 2
Diagnostic Performance of Different Reading Strategies in 55 Patients

Parameter (%)	FDG	FLT	LDCT	FDG + CT	FLT + CT	FDG + FLT	FLT + FDG + CT
Sensitivity	87.5	68.75	68.75	87.50	75.0	81.25	100
Specificity	58.97	76.92	74.36	69.23	87.18	87.18	89.74
Accuracy	67.27	74.45	72.73	74.55	83.64	85.45	92.73
PPV	46.67	55.0	52.38	53.85	70.59	72.22	80.0
NPV	92.0	85.71	85.29	93.1	89.47	91.89	100

LDCT = low-dose CT; PPV = positive predictive value; NPV = negative predictive value.

DISCUSSION

Design of Trial

The limitation of ^{18}F-FDG in the evaluation of lung tumors has been well documented. The reported positive predictive value of ^{18}F-FDG PET or PET/CT in pulmonary lesions was as low as 44.6% (6). ^{18}F-FLT was developed to reflect the proliferation rate of the lesions and to characterize malignant tumor growth (7,8). The current dual-tracer study was designed to prove the following assumptions: (a) ^{18}F-FDG and ^{18}F-FLT provide information relating to different aspects of tumor biology; (b) dual-tracer imaging, with ^{18}F-FDG and ^{18}F-FLT complementary to each other, adds diagnostic confidence; and (c) the criteria in dual-tracer PET/CT image interpretation are objective, accurate, and easy to use. Enormous efforts were taken in this MCCT to avoid known bias that would affect the results.

Comparison of ^{18}F-FLT and ^{18}F-FDG

In most of the cases, ^{18}F-FDG PET detected more lesions than ^{18}F-FLT. The image quality of ^{18}F-FDG was also superior with higher SUVs. The better image quality was believed to be due primarily to its comparatively lower background and more uniform tissue distribution. However, as well described by many authors, nonspecific uptake was noted in a number of benign lesions, especially in tuberculoses. Using $SUV_{MAX} = 2.5$ as the differential threshold, ^{18}F-FDG PET in our study had a fairly low specificity of 58.97% and an accuracy of 67.27%. These figures were lower than those reported earlier (6). The major reason for the lower accuracy was believed to be the relatively higher proportion of TB among the studied subjects, resulting from a higher prevalence of TB in the districts covered by our imaging centers. Another factor to be considered was

that most of our patients had multiple pulmonary nodules. It was recognized earlier that the false-positive rate of ^{18}F-FDG PET was higher in cases of multiple lung lesions (6).

In comparison with ^{18}F-FDG, ^{18}F-FLT images was more "noisy." The positive bone marrow of the thoracic cage interfered with the evaluation of intrathoracic lesions. In most cases, the uptake of ^{18}F-FLT was lower than that of ^{18}F-FDG, which was in accordance with other reports. For example, Buck et al reported that ^{18}F-FLT uptake was only 50% of ^{18}F-FDG uptake in positive nodal metastases of non–small cell lung cancer. ^{18}F-FLT had better specificity (76.92% vs. 58.97%) in our study, but the increased ^{18}F-FLT uptake was not "related exclusively to malignant tumors" as Buck et al. described (5). The uptake of ^{18}F-FLT was present to various degrees in many TB lesions and other benign lesions. This was not entirely unexpected because false-positive ^{18}F-FLT PET had been reported (3,9). The mechanism of false-positive ^{18}F-FLT uptake is poorly understood. We noted that in our patients, the extent of ^{18}F-FLT accumulation in positive benign lesions did not correlate with that of the granulomatous tissue. In our previous in vitro study (Y Tan and J Tian, unpublished data, March 2006), the uptake of ^{18}F-FLT by *Escherichia coli* in the growth phase was 6-fold higher than that of 3 tumor cell lines cultured simultaneously. Yap et al reported a false-positive ^{18}F-FLT PET scan in a case of interstitial pneumonia with a Ki67 of 15% (9). Yamamoto et al. also reported a slightly increased Ki67 (2.6% ± 2.2%) in inflammatory cells (3). Thus, one may postulate that the ^{18}F-FLT uptake could increase in response to active DNA synthesis in any tissue, including growing microbes. The effect of ^{18}F-FLT transportation across cell membranes or a phosphorylation pathway other than thymidine kinase

TABLE 3
χ^2 of Expected Correct and Wrong Reading Counts of Different Strategies

Reading	FDG	FLT	LDCT	FDG + CT	FLT + CT	FDG + FLT	FDG/FLT/CT
Correct	264	260	278	287	259	300	297
Wrong	168	172	154	145	173	132	135

LDCT = low-dose CT.
$\chi^2 = 18.225$, $P = 0.006$.

1 should also be considered (*10,11*). Because of its non-tumor uptake, ^{18}F-FLT might not be suitable to work alone or to replace ^{18}F-FDG in the diagnosis or differentiation of pulmonary lesions.

One problem with ^{18}F-FLT was its fairly low production yield and success rate in synthesis (*7,12*). With the commercially available automatic synthesizer used in our trial, the production succeeded only two thirds of the time, with an average yield of around 13%. The unsatisfactory production efficacy negatively affected the clinical application of the tracer and required improvement of the synthetic techniques (*13*). An unusual high failure rate in synthesis was noted in southern China, which suggested that environmental factors—such as humidity or temperature—might influence the production procedure or the raw materials.

Additional Diagnostic Gains of Dual-Tracer PET

In the current study, ^{18}F-FDG and ^{18}F-FLT images read in pairs helped in establishing the correct interpretation. The ^{18}F-FLT/^{18}F-FDG ratio was more accurate in revealing the nature of the pulmonary pathologies. A ratio between 0.4 and 0.90 depicted most tumors correctly. A similar finding was recognized when the data of previous studies using both ^{18}F-FDG and ^{18}F-FLT were reviewed carefully. Recalculating the assessable data in their studies, we found that the ^{18}F-FLT/^{18}F-FDG ratios in 12 of 18 tumors by Yamamoto et al. (*3*), 8 of 11 tumors by Buck et al. (*5*), and 8 of 12 tumors by Yap et al. (*9*) were in the same range. However, in the study of Cobben et al. (*14*), the ^{18}F-FLT/^{18}F-FDG ratio of malignant lesions was lower, but their late ^{18}F-FDG PET imaging at 90min after injection might result in higher SUV$_{FDG}$—thus, lowering ^{18}F-FLT/^{18}F-FDG ratio. The higher ^{18}F-FLT/^{18}F-FDG ratio in our inflammation was believed to be due to the lower uptake of ^{18}F-FDG by the lesions. Two of 3 benign lesions reported by Yap et al also had ^{18}F-FLT/^{18}F-FDG ratios > 100%.

There was no clear explanation for the different ^{18}F-FLT/^{18}F-FDG ratios among the subgroups of patients. It was known that ^{18}F-FLT is transported into cells via an equilibrative nucleoside transporter–mediated facilitated transport mechanism, phosphorylated by enzyme thymidine kinase 1, and accumulated as mono-, di-, and triphosphate nucleotides in cells (*15*). It might be correct to assume that all of these biochemical processes keep some sort of balance with the energy metabolism of the cells, resulting in a rather fixed ^{18}F-FLT/^{18}F-FDG ratio. The difference in ^{18}F-FLT/^{18}F-FDG SUV ratios between tumors, TB, and inflammation could be useful clinically in separating the different pathologies when neither ^{18}F-FDG nor ^{18}F-FLT could face the challenge alone.

Multimodality imaging has been a hot topic in recent years. Early in 2007, Kim et al. reported that the combination of ^{18}F-FDG PET and CT improved the diagnostic efficacy in solitary pulmonary lesions, with the best performance in ROC analysis (*16*). Another recent report on liver cancer confirmed that dual-tracer PET/CT had an incremental value and a complementary advantage when compared with single-

tracer imaging in the evaluation of metastasis (*17*). In our study, the combination of biologic probes (^{18}F-FDG and ^{18}F-FLT) and of metabolic and anatomic imaging modalities(PET and CT) increased the diagnostic sensitivity and accuracy in a rather heterogeneous group of patients. Two imaging modalities are definitely better than one.

The radiation burden of dual-tracer, dual-modality imaging of the patients must be addressed. The effective dose equivalent of ^{18}F-FLT was estimated by Vesselle et al. (*18*) as 0.031 mSv/MBq (114 mrem/mCi), which is compatible with that of ^{18}F-FDG (0.029mSv/MBq). If 2 doses of 400 MBq were administered in a short interval, the total radiation dose a patient received would be 11.6 + 12.4 = 24 mSv. In view of the potential benefit that the more confident diagnosis could bring to the patients, the dual-tracer strategy should be valued favorably, at least for those with an equivocal diagnosis.

Other Interesting Findings

SUV and Score. In the current study, a good correlation was found between SUV and score for both ^{18}F-FDG and ^{18}F-FLT. It was also shown that the simple scoring based on visual inspection had a diagnostic efficacy similar to that of quantitative SUV. This was in accordance with the reports by Kim et al. (*16*) and Hashimoto et al. (*19*) that semiquantitative means, such as SUV, could hardly add diagnostic value over visual inspection in PET.

Dual-Phase Study. Controversial statements about the usefulness and reliability of delayed imaging of ^{18}F-FDG have appeared in the literature. In our study, the change in SUV between an early scan and a delayed scan was quite unpredictable. It seemed very unlikely to us that the nature of pulmonary lesions could be differentiated satisfactorily on the basis of dual-phase ^{18}F-FDG or ^{18}F-FLT PET.

Value of Low-Dose CT (LDCT). The value of LDCT was appreciated in assisting smaller lesion detection and drawing of ROIs on PET images, especially for ^{18}F-FLT PET. LDCT might miss a few lesions, as O et al (*20*) noted, and the unsatisfactory performance of CT in our study might result from the inclusion criteria that precluded the lesion with typical morphologic features.

Limitations of the Trial. There were several limitations in the design and execution of the current MCCT. First, we used LDCT only; no other classical procedures, such as multiplanar reconstruction or contrast enhancement, were undertaken. This might underestimate the value of CT, although the usefulness of LDCT had been verified previously (*21*). Second, the imaging was acquired and processed using just one model of scanner; the quantitative criteria derived from our study must be cautiously referenced when other devices are used. Third, the number of patients was inadequate, and the composition of diseases was heterogeneous; therefore, not all conclusions may be suitable for the situation in another country or in another study. Because of the limited number of subjects, it was premature to analyze the imaging characteristics according to different histologic

types of tumors or diseases. Fourth, the 1-y follow-up was not long enough. Thus far, we have no data relating to the influence of dual-tracer PET/CT on the long-term clinical outcome of our patients and we have no evidence on the cost-effectiveness of dual-tracer PET/CT. Last, but not the least, the collective blinded reading was organized with readers of different professional backgrounds and inadequate experience and training, and the adjustment of viewing angle and window settings might influence other readers' attention and judgment—therefore, a subjective factor could not be completely excluded.

CONCLUSION

In this prospective, randomized multicenter clinical trial, dual-tracer PET/CT using ^{18}F-FLT and ^{18}F-FDG improved the diagnostic accuracy of differentiating pulmonary nodules. ^{18}F-FLT and ^{18}F-FDG reflected different aspects of biologic features but neither tracer alone could guarantee satisfactory diagnostic performance. Although visual inspection scores worked well as quantitative SUVs for both tracers, the SUV ratio between ^{18}F-FLT and ^{18}F-FDG worked best in the differentiation of malignancies, TB, and other benign lesions. Considering the limited number of patients and the heterogeneity of underling diseases of our study population, the real clinical values, long-term clinical impact, and cost-effectiveness of the dual-tracer PET/CT in the diagnosis of pulmonary nodules are worthy of further investigation.

ACKNOWLEDGMENTS

REFERENCES

1. Strauss LG. Fluoro-18 deoxyglucose and false-positive results: a major problem in the diagnostics of oncological patients. *Eur J Nucl Med.* 1996;23:1409–1415.
2. van Waarde A, Cobben DC, Suurmeijer AJ, et al. Selectivity of ^{18}F-FLT and ^{18}F-FDG for differentiating tumor from inflammation in a rodent model. *J Nucl Med.* 2004;45:695–700.
3. Yamamoto Y, Nishiyama Y, Ishikawa S, et al. Correlation of ^{18}F-FLT and ^{18}F-FDG uptake on PET with Ki-67 immunohistochemistry in non-small cell lung cancer. *Eur J Nucl Med Mol Imaging.* 2007;34:1610–1616.
4. Vesselle H, Grierson J, Muzi M, et al. In vivo validation of 3′-deoxy-3′-[^{18}F]fluorothymidine ([^{18}F]FLT) as a proliferation imaging tracer in humans: correlation of [^{18}F]FLT uptake by positron emission tomography with Ki-67 immunohistochemistry and flow cytometry in human lung tumors. *Clin Cancer Res.* 2002;8:3315–3323.
5. Buck AK, Halter G, Schirrmeister H, et al. Imaging proliferation in lung tumors with PET: ^{18}F-FLT versus ^{18}F-FDG. *J Nucl Med.* 2003;44:1426–1431.
6. Bunyaviroch T, Coleman RE. PET evaluation of lung cancer. *J Nucl Med.* 2006;47:451–469.
7. Shields AF, Grierson JR, Dohmen BM, et al. Imaging proliferation in vivo with [F-18]FLT and positron emission tomography. *Nat Med.* 1998;4:1334–1336.
8. Grierson JR, Shields AF. Radiosynthesis of 3′-deoxy-3′-[^{18}F]fluorothymidine: [^{18}F]FLT for imaging of cellular proliferation in vivo. *Nucl Med Biol.* 2000;27:143–156.
9. Yap CS, Czernin J, Fishbein MC, et al. Evaluation of thoracic tumors with ^{18}F-fluorothymidine and ^{18}F-fluorodeoxyglucose-positron emission tomography. *Chest.* 2006;129:393–401.
10. Reske SN, Deisenhofer S. Is 3′-deoxy-3′-^{18}F-fluorothymidine a better marker for tumor response than ^{18}F-fluorodeoxyglucose? *Eur J Nucl Med Mol Imaging*, 2006;33(suppl 1):38–43.
11. Hinrich A, Wieder HA, Geinitz H, et al. PET imaging with [^{18}F]3′-deoxy-3′-fluorothymidine for prediction of response to neoadjuvant treatment in patients with rectal cancer. *Eur J Nucl Med Mol Imaging.* 2007;34:878–883.
12. Glaser M, Luthro S, Brady F. Applications of positron-emitting halogens in PET oncology. *Int J Oncol.* 2003;22:253–267.
13. Oh SJ, Mosdzianowski C, Chi DY, et al. Fully automated synthesis system of 3′-deoxy-3′-[18F]fluorothymidine. *Nucl Med Biol.* 2004;31:803–809.
14. Cobben DC, Elsinga PH, Hoekstra HJ, et al. Is ^{18}F-3′-fluoro-3′-deoxy-L-thymidine useful for the staging and restaging of non-small cell lung cancer? *J Nucl Med.* 2004;45:1677–1682.
15. Grierson JR, Schwartz JL, Muzi M, et al. Metabolism of 3′-deoxy-3′-[F-18]fluorothymidine in proliferating A549 cells: validations for positron emission tomography. *Nucl Med Biol.* 2004;31:829–837.
16. Kim SK, Allen-Auerbach M, Goldin J, et al. Accuracy of PET/CT in characterization of solitary pulmonary lesions. *J Nucl Med.* 2007;48:214–220.
17. Ho CL, Chen SR, Yeung DWC, et al. Dual-tracer PET/CT imaging in evaluation of metastatic hepatocellular carcinoma. *J Nucl Med.* 2007;48:902–909.
18. Vesselle H, Grierson J, Peterson LM, Muzi M, Mankoff DA, Krohn KA. ^{18}F-Fluorothymidine radiation dosimetry in human PET imaging studies. *J Nucl Med.* 2003;44:1482–1488.
19. Hashimoto Y, Tsujikawa T, Kondo C, et al. Accuracy of PET for diagnosis of solid pulmonary lesions with ^{18}F-FDG uptake below the standardized uptake value of 2.5. *J Nucl Med.* 2006;47:426–431.
20. O JH, Yoo IR, Kim SH, et al. Clinical significance of small pulmonary nodules with little or no ^{18}F-FDG uptake on PET/CT images of patients with nonthoracic malignancies. *J Nucl Med.* 2007;48:15–21.
21. Schöder H, Yeung HWD, Larson SM. CT in PET/CT: essential features of interpretation. *J Nucl Med.* 2005;46:1249–1251.